Assessment of Magic Angle Spinning Spectroscopy
for Studying Migration in Solid Milk Chocolate

by

Dwight McCoy Chambers

SUBMITTED TO THE DEPARTMENT OF NUCLEAR SCIENCE AND ENGINEERING IN PARTIAL FULFULLMENT OF THE REQUIREMENTS FOR THE DEGREE OF

BACHELORS OF SCIENCE IN NUCLEAR SCIENCE AND ENGINEERING
AT THE
MASSACHUSETTS INSTITUE OF TECHNOLOGY

JUNE 2007

Signature of Author: _____
Department of Nuclear Science and Engineering
May 21, 2007

Certified by: _____
David Cory
Professor of Nuclear Science and Engineering
Thesis Supervisor

Accepted by: _____
David Cory
Professor of Nuclear Science and Engineering
Chairman, NSE Committee for Undergraduate Students

Assessment of Magic Angle Spinning Spectroscopy
for Studying Migration in Solid Milk Chocolate

by

Dwight McCoy Chambers

Submitted to the Department of Nuclear Science and Engineering on May 21, 2007
In Partial Fulfillment of the Requirements for the Degree of
Bachelor of Science in Nuclear Science and Engineering

Abstract

In the confectionery industry, there is considerable interest in understanding the mechanisms of liquid lipid migration inside chocolates as it relates to combating fat-bloom defects in confectionery products. [1] This thesis investigates the ability of MAS NMR spectroscopy to adequately resolve chocolate spectra and deliver diffusion data specific to individual chemical species. Using a Bruker 300 MHz spectrometer equipped with liquid state and hr-MAS probes various spectroscopic characteristics of a milk chocolate sample were recorded. The MAS spectrometer resolved the chocolate spectrum into individual chemical signals and demonstrated multi-compartment diffusion behavior.

Thesis Supervisor: David Cory
Title: Professor of Nuclear Science and Engineering

Table of Contents

Abstract	2
List of Figures	4
List of Tables	5
1. Introduction	6
1-1. NMR Spectroscopy of Chocolates and the Fat Blooming Phenomena	6
1-2. Magic Angle Spinning (MAS) Spectroscopy of Solids in NMR	7
1-3. Stimulated Echo and its Application to Diffusion Measurements	8
2. Methodology	10
2-1. Sample Preparation	10
2-2. T1, T2, and Diffusion NMR Experiments	10
2-3. MAS NMR Experiments	12
3. Data Analysis and Results	14
3-1. Gross Sample Relaxation Characteristics and Diffusion Behavior	14
3-2. MAS NMR Spectrum and Diffusion Measurements	16
4. Discussion	19
5. Conclusions	20
References	21
Acknowledgments	22

List of Figures

Figure 1: Cartoon of chocolate 6
Figure 2: Visual comparison of normal milk chocolate and milk chocolate with fat bloom 6
Figure 3: Illustration of sample in MAS configuration 8
Figure 4: Generalized Stimulated Echo with Continuous Gradient 9
Figure 5: Inversion recovery sequence 10
Figure 6: CPMG sequence 11
Figure 7: Stimulated echo sequence 12
Figure 8: MAS stimulated echo sequence 13
Figure 9: Plot of Z(t) versus the D2 delay from the inversion recovery sequence 15
Figure 10: Plot of Max Observed Signal versus Total Relaxation Time 15
Figure 11: Observed Signal versus Gradient Strength for Gross Diffusion Behavior 16
Figure 12: NMR Spectrum of the Stationary Sample 17
Figure 13: Chocolate MAS Spectrum at 3 kHz 17
Figure 14: MAS Diffusion Spectrum with 10% MA Gradient 18
Figure 15: MAS Diffusion Spectrum with 20% MA Gradient 18

List of Tables

Table 1:Inversion Recovery Experiment Parameters 11
Table 2: CPMG Experiment Parameters 11
Table 3:Stimulated Echo Experiment Parameters 12
Table 4:MAS Stimulated Echo Experiment Parameters 13
Table 5: FWHM of MAS Spectrum Peaks 16

1. Introduction

1-1. NMR Spectroscopy of Chocolates and the Fat Blooming Phenomena

Chocolate is a complex composite food composed of a matrix of cocoa, sugar and milk awash in a sea of liquid fats. [1] The behavior of this composite (depicted in the cartoon in Figure 1) is extremely sensitive to many factors including processing techniques, temperature, and the proximity of foreign liquid fats in composite foods. [1, 2]

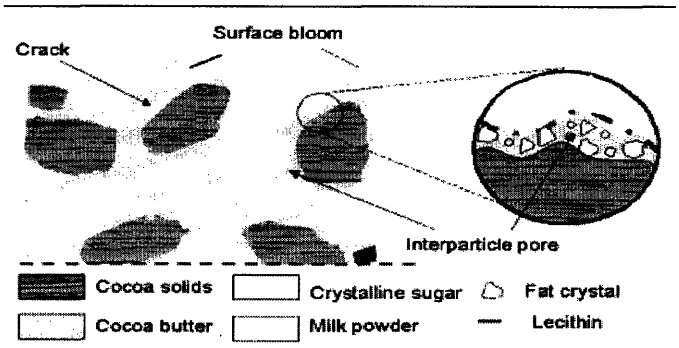

Figure 1: Cartoon of chocolate [1]

Many food scientists and companies have studied chocolate using NMR spectroscopy, and a significant portion of this research has been dedicated to studying the migrations of lipids inside chocolate. [1-3] This research is often motivated by a desire to understand the underlying mechanisms causing "fat-blooms" - a chocolate blight in which lipids migrate to the surface of the chocolate, causing a white discoloration and poor taste. [4] An example of fat bloom can be seen on the surface of the right chocolate bar in Figure 2.

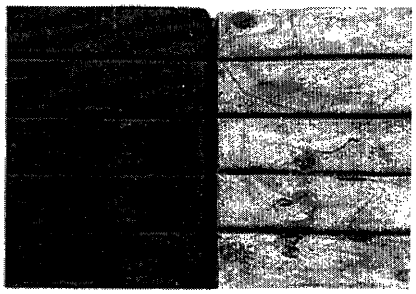

Figure 2: Visual comparison of normal milk chocolate and milk chocolate with fat bloom [4]

Initially, researchers tried to explain lipid migratory behavior solely in terms of molecular diffusion. Now, there is an emerging view of the mechanistic foundations of fat-blooming in which the phenomena is a combination of molecular diffusion and capillary action. [1, 3] In order to further clarify the matter, it may be helpful to scientists to be able to more accurately track the migration of individual chemical species through chocolates. This thesis will examine the suitability of using MAS NMR spectroscopy in order to study the migratory behavior of individual chemical species in chocolates. Specifically, this study will assess whether MAS NMR techniques can accurately resolve a chocolate spectrum with enough sensitivity so as to pick out individual species migratory behavior.

1-2. Magic Angle Spinning (MAS) Spectroscopy of Solids in NMR

MAS spectroscopy is a technique used in NMR to acquire high resolution spectra in solid state systems. [5-6] In all media, there are dipole interactions between nuclei. In a general magnetic field, the dipole interaction between any two nuclei, i and j, at a distance R from each other, and where the vector R is at an angle Θ to the magnetic field, is proportional to:

$$\left(\frac{1}{R_{ij}^3}\right)(3*\cos(\Theta)^2-1) \qquad \text{(Equ. 1)} \quad [6]$$

In many solutions, the random motion and rotational freedom on the nuclei cancel out any net dipole interactions for the solution. However, in solid state systems, the nuclei are often much more constrained both translationally and rotationally. The presence of dipole interactions generally leads to broad line widths in NMR spectroscopy. [5,6]

Many of the interactions averaged out by MAS in composite systems such as chocolate arise from the inherent heterogeneity of bulk magnetic susceptibility in the sample. This is a reflection of the fundamental compositional heterogeneity and the differing magnetic susceptibilities of each individual component of the sample composite. [9] The effective magnetic field is thus spatially dependent, receiving contributions from the magnet's static field, B_0, and the local field variations as shown in Equation 2:

$$B_{eff} = B_0 + B_{loc} \qquad \text{(Equ. 2) [9]}$$

MAS spectroscopy exploits the angular dependence of this phenomena in order to address the limited motion of solid state nuclei by rapidly rotating the sample about an axis which is 54.74° with respect to the orientation of the magnetic field as shown in Figure 3. [5,6]

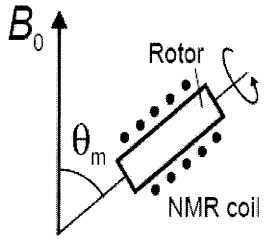

Figure 3: Illustration of sample in MAS configuration [5]

Through sufficiently rapid rotation of the sample, the average NMR frequency suppresses the dipole interactions and varying magnetic susceptibilities of the constituent parts, resulting in a solution like spectrum. [5,6] The extent of the narrowing achieved in an NMR spectrum by MAS spectroscopy is dependent on the rate of spinning of the sample. [6]

1-3. Stimulated Echo and Its Application to Diffusion Measurements

Given the desire to study diffusion behavior in chocolate, it is important to choose a pulse sequence which can adequately highlight its affect on the signal. In NMR, the attenuation of a signal by molecular diffusion is a function of essentially two properties of a pulse sequence: the amount of time the nuclei are left to diffuse (storage time) and the "steepness" of the phase encoding done by the gradient (which is to say the product of the gradient strength and the gradient's application time). [6] The stimulated echo is a simple pulse sequence which gives a researcher broad flexibility in adjusting all three of these features so as to maximize their ability to measure diffusion.

The sequence is depicted schematically in Figure 4 (Figure 4 represents a generic version of the stimulated echo sequence but all discussion related to Figure 4 will apply generically to those other

possible versions as well). The three π/2 pulses are separated by two delays, t and T. These delays represent the gradient application time and the spin storage time respectively. Also shown in Figure 4 are the 5 echoes that form as a result of this pulse sequence – 1,3,4 and 5 are simple spin echoes while 2 is the stimulated echo which occurs 2t+T after the initial pulse. [7-8]

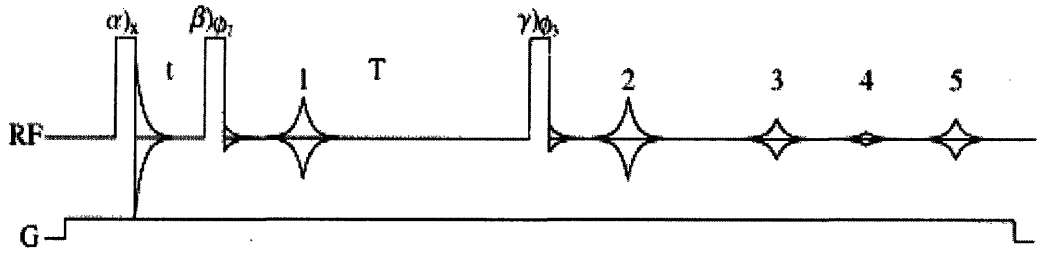

Figure 4: Generalized Stimulated Echo with Continuous Gradient [7]

The stimulated echo is different from the 4 other echoes because it spends the T delay along the B_0 axis, and accordingly only undergoes T_1 and not T_2 relaxation during that period. [7-8] Since the T_1 is necessarily larger than T_2, these spins are substantially less attenuated upon refocusing into an echo. [6-8] This helpful feature of the sequence frees the researcher from T_2 constrains which might otherwise severely limit the possible storage time. [7-8] It is also worth noting that the research maintains broad control over the gradient strength and gradient application time in the stimulated echo sequence.

2. Methodology:

2-1. Sample Preparation

A sample of Flyer Swiss milk chocolate was acquire from a local food store. For the early NMR experiments, a portion of this sample was cut off and loaded into an NMR sample tube (Wilmad-Labglass product 504-PP-9) which was then sealed with a rubber cap. For the later MAS experiments, a second sample was prepared from the remaining chocolate originally purchased. This sample was tightly packed into a ceramic MAS rotor (Bruker hr-MAS product B200147) with the use of a plunger so as to remove any possible voids in the chocolate. This rotor was then sealed as well.

2-2. T_1, T_2, and Diffusion NMR Experiments

These experiments were conducted using a 300 MHz Bruker NMR Spectrometer using a SEI 300 MHz probe in Prof. David Cory's laboratory at the Massachusetts Institute of Technology. The π and $\pi/2$ pulses were determined to be 22.85 us and 11.42 us respectively. In order to measure the spin-lattice (T_1) relaxation time of the sample, an inversion recovery sequence, shown in Figure 5, was used.

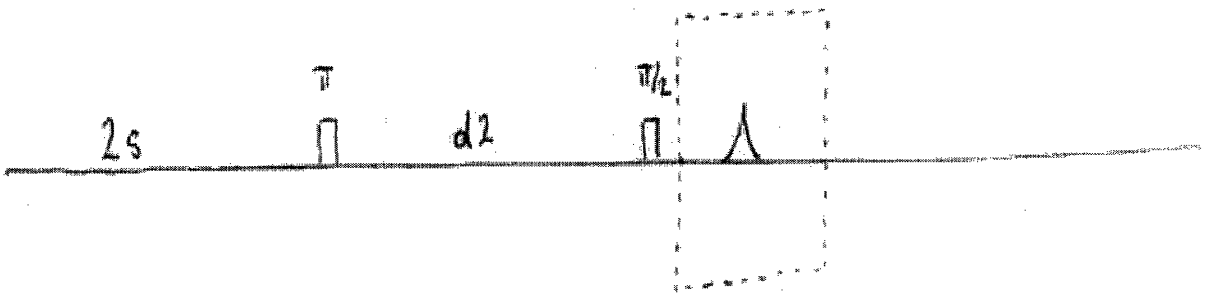

Figure 5: Inversion recovery sequence

The experimental parameters for the 11 inversion recovery experiments are summarized in Table 1.

Experiment	D1 (s)	D2 (ms)	P1 (us)	P2 (us)	Pulse Power (db)	Dwell Time (us)
IR-1	3	10	22.85	11.42	2	10
IR-2	3	50	22.85	11.42	2	10
IR-3	3	100	22.85	11.42	2	10
IR-4	3	200	22.85	11.42	2	10
IR-5	3	275	22.85	11.42	2	10
IR-6	3	300	22.85	11.42	2	10
IR-7	3	400	22.85	11.42	2	10
IR-8	3	500	22.85	11.42	2	10
IR-9	3	600	22.85	11.42	2	10
IR-10	3	800	22.85	11.42	2	10
IR-11	3	1000	22.85	11.42	2	10

Table 1: Inversion Recovery Experiment Parameters

In order to characterize the spin-spin relaxation time (T_2), a CPMG sequence, which is shown generically in Figure 6, was used. The experimental parameters for the 8 CPMG experiments are summarized in Table 2.

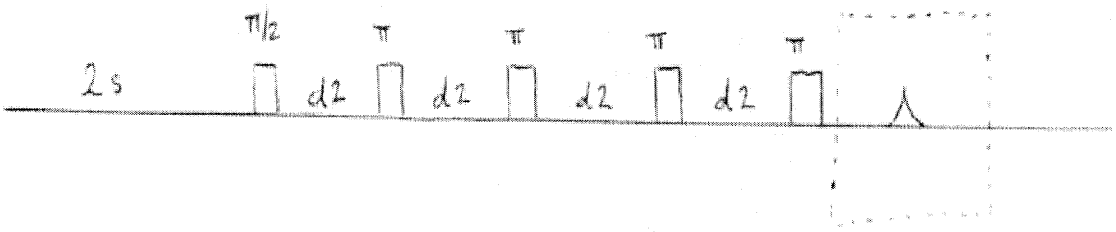

Figure 6: CPMG sequence

Experiment	D1 (s)	D2 (us)	P1 (us)	P2 (us)	Pulse Power (db)
CPMG-1	2	100	11.42	22.85	2
CPMG-2	2	200	11.42	22.85	2
CPMG-3	2	300	11.42	22.85	2
CPMG-4	2	600	11.42	22.85	2
CPMG-5	2	900	11.42	22.85	2
CPMG-6	2	1000	11.42	22.85	2
CPMG-7	2	1500	11.42	22.85	2
CPMG-8	2	2000	11.42	22.85	2

Table 2: CPMG Experiment Parameters

In order to assess the bulk diffusion characteristics of the sample, a stimulated echo sequence, which is shown in Figure 7, was used. The experimental parameters for the stimulated echo experiments are reported in Table 3.

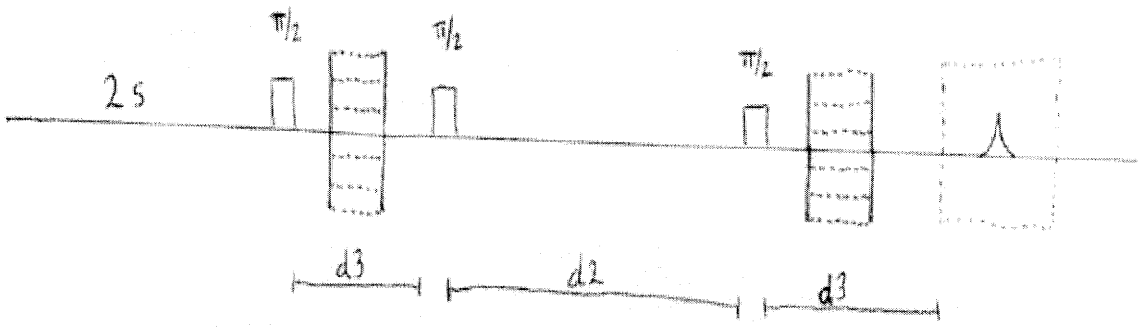

Figure 7: Stimulated echo sequence

Experiment	D1 (s)	D2 (us)	D3 (us)	Gradient Strength (%)
D-1	2	437.9	700	20
D-2	2	437.9	700	25
D-3	2	437.9	700	35
D-4	2	437.9	700	50

Table 3: Stimulated echo experiment parameters

2-3. MAS NMR Experiments

All MAS experiments were conducted using a hr-MAS Bruker probe in the same 300 MHz system as the relaxation experiments. After loading the MAS sample rotor, the sample was spun in the probe at 3 kHz. The π and $\pi/2$ pulses were 9 us and 18 us, respectively. A simple spectrum of the sample was acquired by using a hard $\pi/2$ pulse. The MAS diffusion spectra were acquired using a modified version of the earlier stimulated echo sequence and is shown in Figure 8. The experimental parameters are reported in Table 4.

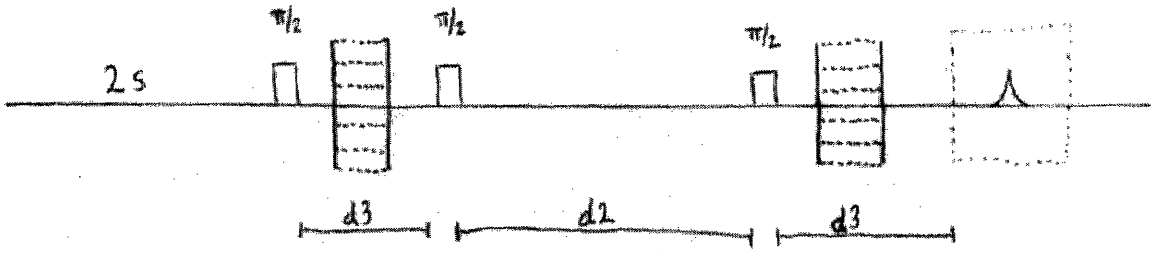

Figure 8: MAS stimulated echo sequence

Experiment	D1 (s)	D2 (ms)	D3 (ms)	Gradient Strength (%)
MAS D-1	2	10	400	10
MAS D-2	2	10	400	20

Table 4: MAS stimulated echo experiment parameters

3. Data Analysis and Results

3-1. Gross Sample Relaxation Characteristics and Diffusion Behavior

In an inversion recovery experiment, the amplitude of the FID signal, M_{T1}, is:

$$M_{TI}(t)=M_0*(1-2*e^{-t/T_1}) \qquad \text{(Equ. 3) [6]}$$

where t is the delay between the initial π pulse and the subsequent $\pi/2$ pulse, and M_0 is the initial magnetization at t = 0. It is possible to rewrite Equation 3 so that:

$$Z(t)=\frac{1}{2}(1-M_{TI}(t)/M_0)=e^{-t/T_1} \qquad \text{(Equ. 4)}$$

After fitting the experimental results, shown in Figure 9, to a simple exponential curve, the T_1 value can be measured directly from the fit. The measured T_1 value for this chocolate sample is 456 ms.

In a CPMG sequence, amplitude of the FID signal, M_{T2}, is a function of the total time, t, spent in plane transverse to the B_0 field and the initial magnetization of the sample M_0. In the simplest case, the relationship is a simple exponential decay as shown in Equation 5:

$$M_{T2}(t)=M_0*e^{-t/T_2} \qquad \text{(Equ. 5) [6]}$$

Using a best fit line for the experimental data shown in Figure 10, the measured T_2 value for the chocolate sample is 6.12 ms.

Finally, the signal amplitude in the pulsed gradient diffusion experiment is a function of the gradient strength, the gradient application time (D3 from Table 3) and the storage time (D2 from Table 3):

$$M(G,D2,D3)=M_0*(e^{-D*G^2*D2^2*\gamma^2*(D3+(\frac{2}{3})*D2)}) \qquad \text{(Equ. 6) [6]}$$

where D is the molecular diffusion coefficient of the mobile species. By taking the natural log of the observed signal's maximum, the linear best fit in Figure 11 estimates the diffusion coefficient of the mobile species in the chocolate to be 2.87 $\mu m^2/ms$.

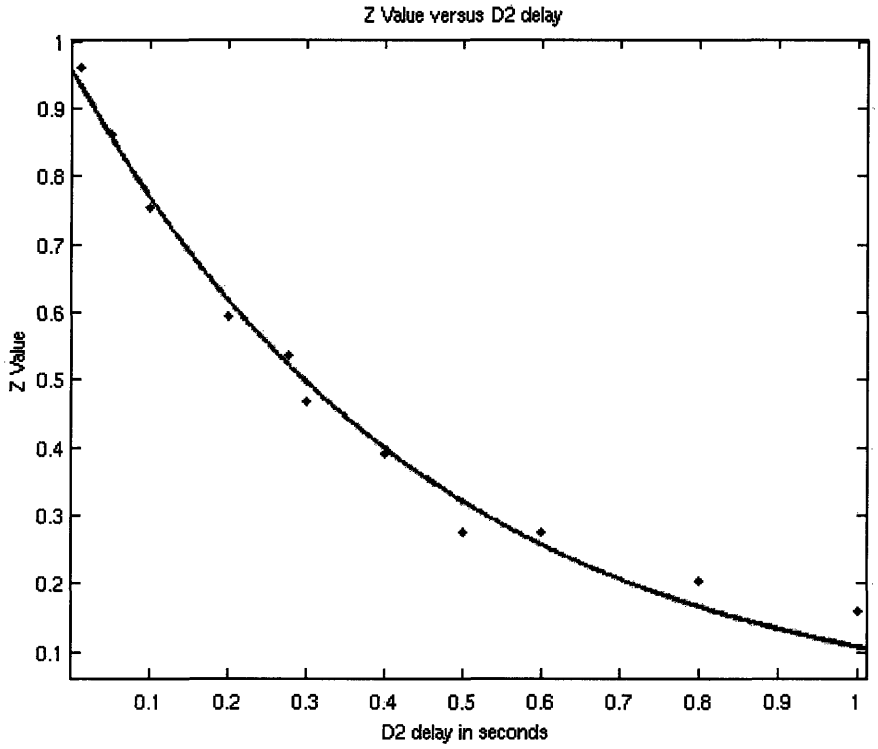

Figure 9: Plot of Z(t) versus the D2 delay from the inversion recovery sequence

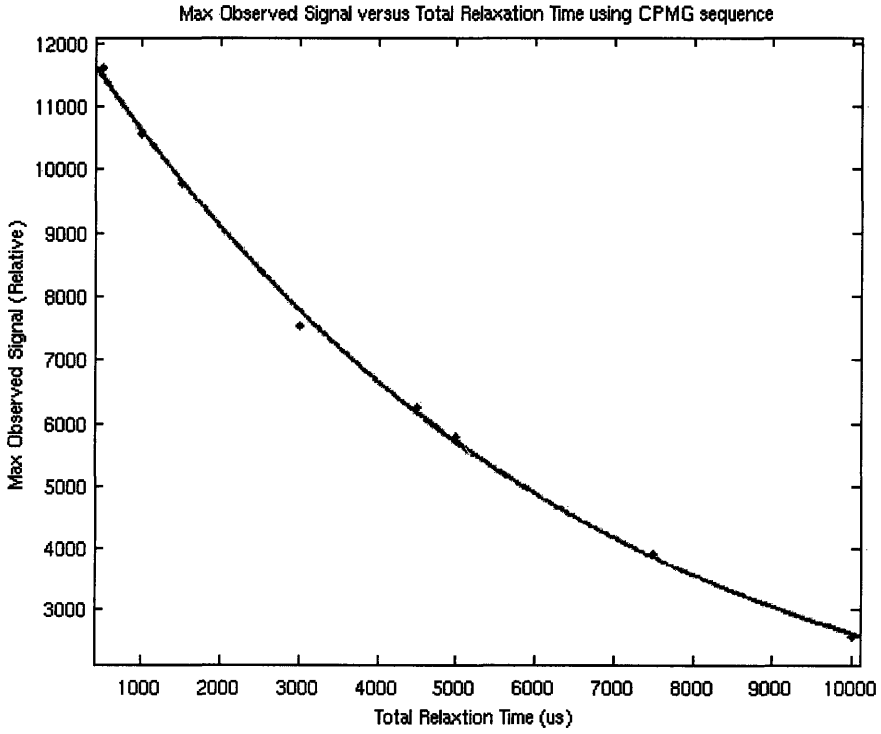

Figure 10: Plot of Max Observed Signal versus Total Relaxation Time

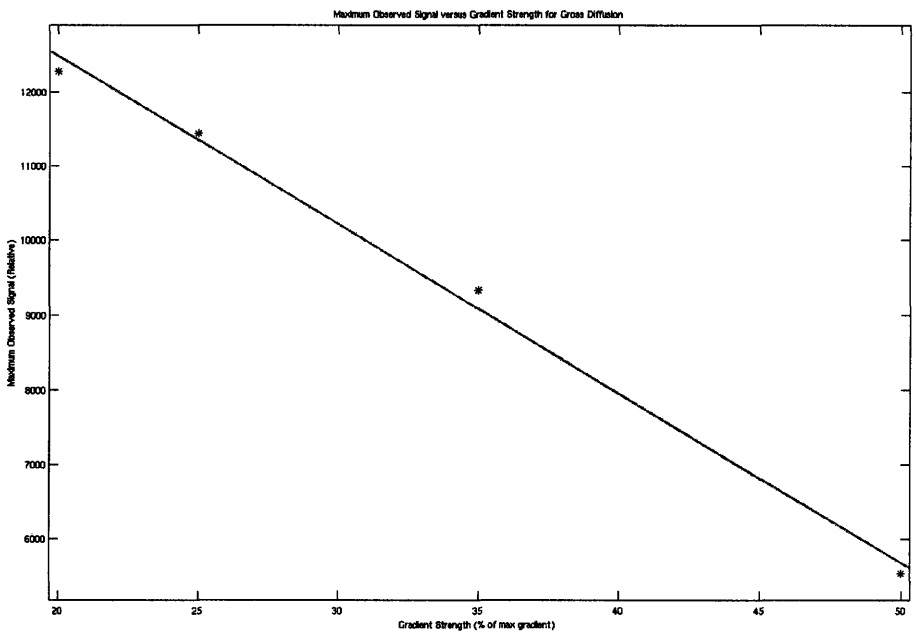

Figure 11: Maximum Observed Signal versus Gradient Strength for Molecular Diffusion Behavior

3-2. MAS NMR Spectrum and Diffusion Measurements

Using the liquid state probe, the chocolate spectrum was dominated by a single peak with a full-width-half-maximum (FWHM) of 2.196 ppm. The peak, shown in Figure 12, has a generally Lorentzian line-shape with the obvious exception of the subsumed peak on the left. At 3 kHz in the hr-MAS probe, the chocolate's spectrum breaks into 9 distinguishable peaks as can be seen in Figure 13 The FWHM of peak of the 9 peaks are listed in Table 5 with Peak 1 on the right.

Peak	1	2	3	4	5	6	7	8	9
Resonant Frequency (ppm)	0.641	1.047	1.324	1.763	1.991	2.536	3.821	4.016	5.066
Spectrum FWHM (ppm)	0.105	0.114	0.146	0.130	0.114	0.097	0.122	0.114	0.114
Diffusion (14) Spectrum FWHM (ppm)	0.181	0.249	N/A	N/A	N/A	N/A	N/A	N/A	0.206

Table 5: Peak Information for MAS Spectrum and MAS Diffusion Spectrum

Figures 14 and 15 show the resulting chocolate MAS spectra using the pulse sequence from Figure 8 and the experimental parameters listed in Table 4. Despite the two-fold increase in gradient strength between trials, there is no significant change to the spectrum from additional diffusion.

There are also several noteworthy contrasts between the MAS spectra in Figures 13 and 14.

Most, notably, the signal in Figure 14 is weaker, more noisy and has worse resolution. There are also prominent spinning sidebands present in Figure 13 at 11.020 ppm and -9.007 ppm which are absent in Figure 14 and 15.

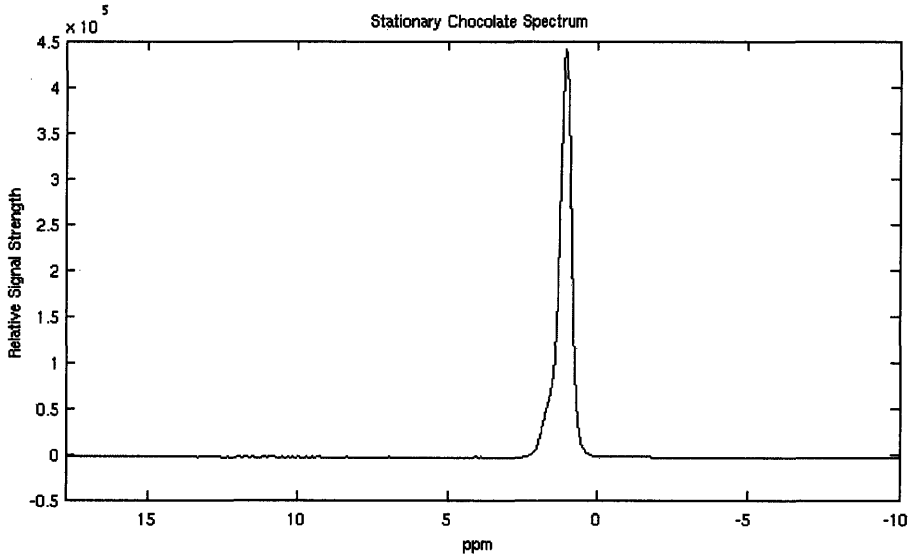

Figure 12: NMR Spectrum of the Stationary Sample

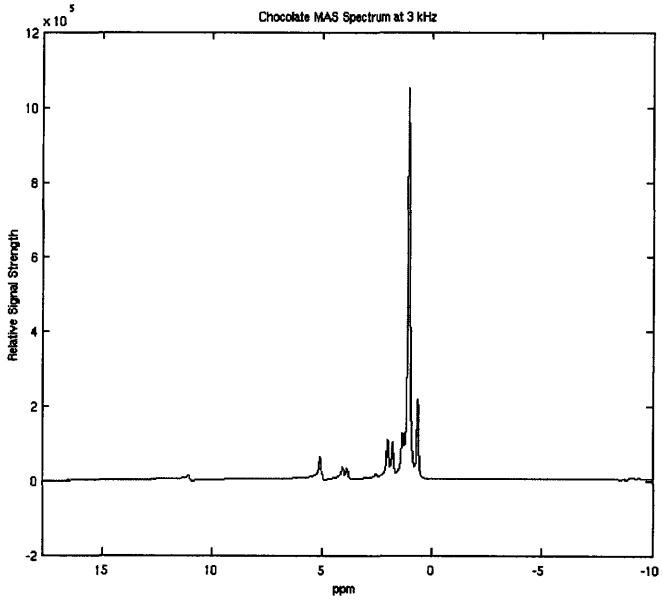

Figure 13: Chocolate MAS Spectrum at 3 kHz

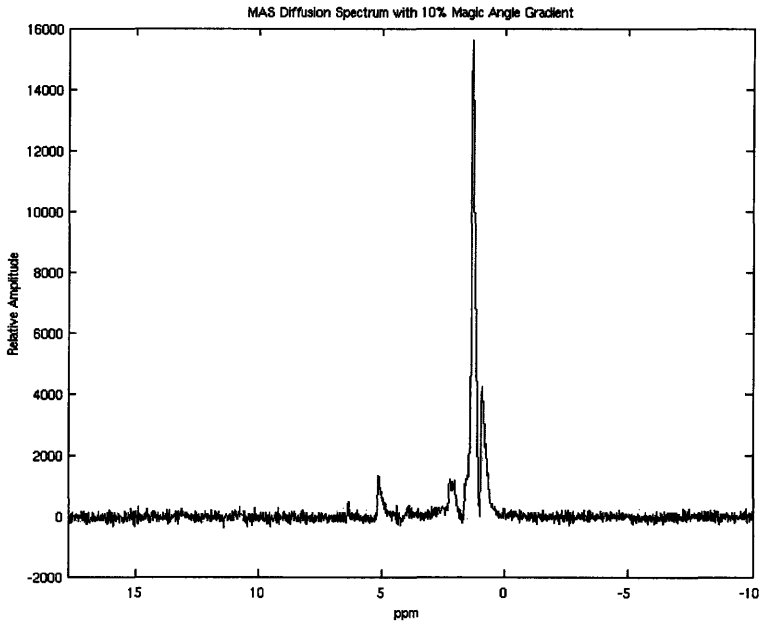

Figure 14: MAS Diffusion Spectrum with 10% MA Gradient

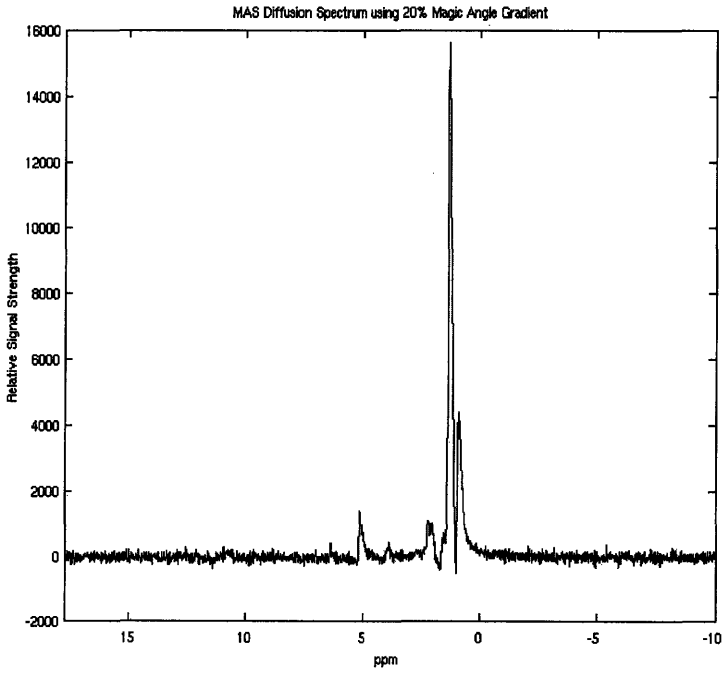

Figure 15: MAS Diffusion Spectrum using 20% Magic Angle Gradient

4. Discussion

The two spectra in the Results section from the MAS and liquid state probes quite clearly illustrate the ability of MAS NMR spectroscopy to return a high resolution spectrum of a solid-state sample. MAS, even at a modest spinning rate, quite clearly reduced the chocolate spectrum from a single lumped, broad signal to its fundamental component peaks. Using the chemical shift data stored in Figure 13, it is possible to assign each peak to particular chemical species present in chocolate – thus, fulfilling the first expectation of the MAS assembly.

In order to address the needs of researchers further exploring lipid migration in chocolate, the MAS assembly also needed to be able to study the migration behavior of individual species. The MAS spectra in Figure 13, 14 and 15 clearly report on diffusion behavior of two distinct groups within the chocolate: a liquid-like group and a solid state group. The solid state group is restricted in its mobility, while the liquid state is much less constrained. Evidence for the mobility restriction of the solid state comes from the comparison of Figures 14 and 15 in which a significant increase in gradient strength did not attenuate signal strength, indicating a population unable to diffuse.

The apparent mobility of the liquid like spins can be seen both in the presence of spinning sidebands in Figure 13 [9], as well as the contrast between the smooth sharp peaks in Figure 13 and the broader, nosier peaks in Figure 14. Referring to Table 5, the FWHM about doubled in all cases between Figures 13 and 14. This is most likely a reflection of the diversity of the chemical environments seen by the stationary sample in Figure 14. Each differing environment should shift (minutely in this case) the peaks , resulting in broader, nosier peaks. While the solid state behavior is also present in Figure 13, it is masked by the presence of the liquid state population (which had been attenuated by the diffusion experiments in Figure 14). The mobility of the liquid phase spins allows them to sample many different chemical environments – averaging out this shifting and resulting in smoother, narrower lines.

5. Conclusions

MAS spectroscopy is capable of resolving the chocolate spectrum into its component peaks, and during investigation of diffusion behavior in the chocolate, MAS spectroscopy was able to clearly identify two unique populations within the sample. Future work in the area should focus on identifying potential species involved in both a diffusion and capillary action model of fat blooming. Having developed theoretical models, scientists could use the species specific migration data from potential future MAS NMR spectroscopy experiments to evaluate the validity of such models. Beyond information on the behavior of individual species, the liquid state population, in particular, may also be a source of valuable information about the characteristic spaces inside the chocolate. Information about the geometry of the chocolate matrix may also help researchers refine their models.

References

[1] Aguilera, J.M., Michel, M., and G. Mayor, "Fat Migration in Chocolate: Diffusion or Capillary Flow in a Particulate Solid?- A Hypothesis Paper," Journal of Food Science, Vol. 69, Nr. 7, pp. 167-174, 2004.

[2] Walter, Peggy and Paul Cornillon, "Lipid migration in two-phase chocolate systems investigated by NMR and DSC," Food Research International, Volume 35, pp 761-767, 2002.

[3] Guiheneuf, T.M., Couzens, P. J, Wille, H. J., and L. Hall, "Visualization of Liquid Triacylglycerol Migration in Chocolate by Magnetic Resonance Imaging," Journal of the Science of Food and Agriculture, Vol. 73, Issue 3, pp. 265-273, 1999.

[4] R. Peschar, M.M. Pop, D.J.A. De Ridder, J.B. Van Mechelen, R.A.J. Driessen, H. Schenk, "Structure of Chocolate Clarified with Synchrotron Powder Diffraction Data," J. Phys. Chem. B., Vol. 108, Nr. 40, pp. 15450-15453, 2004.

[5] Jeschke, G. "High-Resolution Solid-State NMR: Magic Angle Sample Spinning and Cross Polarization," Lecture Notes: www.mpip-mainz.mpg.de/~jeschke/lect9.pdf, 2004.

[6] Fukushima, Elichi and Stephen B.W. Roeder, Experimental Pulse NMR: a Nuts and Bolts Approach, Addison-Wesley Publishing Company: Reading, MA, 1993.

[7] Sodickson, A and David Cory, "A generalized k-space formalism for treating spatial aspects of a variety of NMR experiments," Progress in Nuclear Magnetic Resonance Spectroscopy, Vol. 33, pp. 77-108, 1998.

[8] Cho, Z.-H., Jones, J. P., and Manbir Singh, Foundations of Medical Imaging, John Wiley & Sons, Inc.: New York,1993.

[9] Liu, Y., Gabriela, L., Singer, S., Cory, D., and Pabitra Sen, "Manipulation of phase and amplitude modulation of spin magnetization in magic angle spinning nuclear magnetic resonance in the presence of molecular diffusion," Journal of Chemical Physics, Vol 114, Nr. 13, 2001.

Acknowledgments

The author would like to thank the following people: Prof. Cory time and effort spent advising me during this project and for the use of your lab equipment; Sekhar for the sound advice, the technical assistance with the probes and the Nuts and Bolts; Jonathan, for his help with all things Athena and printing, Troy for a through introduction to experimental NMR, and Michael for patent advice, catching typos in the first line of my abstract and laughing at my numerous chocolate jokes which sadly never made it into this thesis.